SINR Prediction in Mobile CDMA Systems by Linear and Nonlinear Artificial Neural-Network-Based Predictors

Nahid Ardalani[1]
[1] **Electrical Engineering Department, Islamic Azad University, Central Tehran Branch, Tehran, Iran**

Abstract

This article describes linear and nonlinear Artificial Neural Network(ANN)-based predictors as Autoregressive Moving Average models with Auxiliary input (ARMAX) process for Signal to Interference plus Noise Ratio (SINR) prediction in Direct Sequence Code Division Multiple Access (DS/CDMA) systems. The Multi Layer Perceptron (MLP) neural network with nonlinear function is used as nonlinear neural network and Adaptive Linear (Adaline) predictor is used as linear predictor. The problem of complexity of the MLP and Adaline structures is solved by using the Minimum Mean Squared Error (MMSE) principle to select the optimal numbers of input and hidden nodes by try and error role. Simulation results show that both of MLP and Adaline optimal neural networks can track the effect of deep fading due to using a 1.8 GHZ carrier frequency at the urban mobile speeds of 10 km/h, 50 km/h and 120 km/h with tolerable estimation errors. Therefore, the neural network-based predictor is well suitable SINR-based predictor in closed-loop power control to combat multi path fading in CDMA systems.

Keywords: *Neural Networks, DS/CDMA, Multi Path Fading Channel, Closed-Loop Mobile Power Control, SINR Prediction, Neural Network Optimization.*

1. Introduction

In present mobile communication systems there are many new technologies emerging to improve transmission and reception techniques of digital symbols over a fading channel. These new technologies include smart antenna [1], transmitter/receiver diversity [4], interference cancellation [2], and power control [3]. Closed-loop power control and feedback procedure is crucial in the uplink transmission (from mobile to base station) to control mobile's signal transmission power by sending power control commands from base station to either lower or higher transmitting power level for each user independently to keep the received power level from each mobile unit equal and constant in the average [5], [6], [7]. There are two problems encountered in the power control scheme. One is the time varying statistics of fading loss and interference since they are hard to estimate. The other is the round-trip delay which made degrade the system performance or even lead to instability of the closed-loop power control system [8], [9]. A robust power control algorithm based on linear quadratic control theory and Kalman filter is proposed in [10], [11]. On the other hand, to learn the time-varying channel fading and interference, several adaptive minimum variance controllers [12],[13] have been developed with superior performance to the conventional power control methods [14]. Power control based on the Fuzzy control approach can be found in [15]. The capacity and quality of service (QOS) of CDMA systems greatly depends on the mobile power control function. While an open-loop power control can solve the near-far and shadowing problems [16], [17], the closed-loop power control can combat multi path fading [18]. The inherent problem in a closed-loop power control algorithm is feedback delay. The utility optimization and target SINR tracking can be achieved at the same time by using the adaptive algorithm through the net utility function based on QOS for the purpose of resource management of wireless communication networks [19]. In this situation the information of power control command is outdated and not reliable. We need to predict the value of signal strength or SIR at the time that the power control commands should actually take place [21], [20]. The closed-loop power control with predictive SINR estimation is illustrated in Fig.1. The estimator in the base station can either estimate the received signal strength or the SINR [22], [23], [24]. In addition power control based on SINR is more suitable than that based on signal strength because CDMA is interference limited [25], [26]. A hybrid and modified Elmann neural networks and Heinonen-Neuvo prediction were proposed in [27], [28] to predict signal strength and they used Predictive Minimum Description Length (PMDL) method to find the optimal neural Network [29], [30].

In this paper the structure of MLP predictor is first optimized off-line and the performance of all mentioned structures are evaluated in terms of bias and mean squared error (MSE) then use the optimal predictor with on-line learning and adaptation in the real situation[31],[32]. In section 2 a daptive predictors and back propagation algorithm in ANN are discussed. In section 3 a Rayleigh fading channel simulator and SINR estimator technique are described. In section 4 we discuss the topology of feed forward neural network-based power prediction and the applied learning algorithm. The optimized neural predictor is found off-line and applied to predict SINR in a Rayleigh fading channel. An illustrative simulation is demonstrated in section 5. Finally we conclude this paper with a few remarks and discussion in section 6.

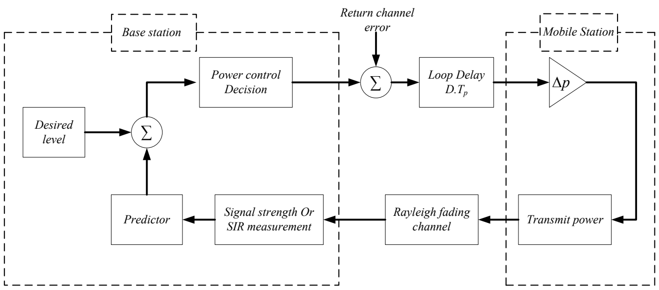

Fig.1 Closed-loop power control model

2. Adaptive Predictors

The structure of the Adaptive Filter is shown in block diagram form in Fig.2. In consists of two basics parts:(1) a transversal filter with adjustable tap weights whose values at time n are denoted $w_1(n), w_2(n), \ldots, w_M(n)$ and (2) a mechanism for adjusting these tap weights in an adaptive manner [33], [34]. During the filtering process if the tap an additional response, called the desired response, is supplied along with the usual tap inputs.

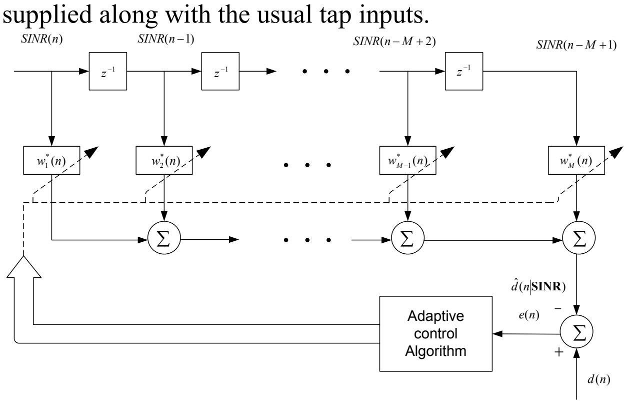

Fig. 2 Adaptive Filter in predictor application with SINR input

In effect, the desired response provides a f rame of reference for adjusting the tap weights of filter. We may thus write:

$$e(n) = SINR(n+1) - S\hat{I}NR\big(n \big| \mathbf{SINR}\big)$$
$$= SINR(n+1) - \mathbf{w}^{\mathbf{H}}(n)\mathbf{SINR}(n) \quad (1)$$

The term $\mathbf{w}^{\mathbf{H}}(n)\mathbf{SINR}(n)$ is the inner product of the tap-weight vector $w(n)$ and the tap-input vector $\mathbf{SINR}(n)$. The expanded form of the tap-weight vector is described $\mathbf{w}^T(n) = [w_1(n), w_2(n), \cdots, w_M(n)]$ and that of the tap-input vector by $\mathbf{SINR}(n) = [SINR(n), SINR(n-1), \ldots, SINR(n-M+1)]$. If the tap-input vector $\mathbf{SINR}(n)$ and the described are jointly stationary, then the mean squared error $\mathbf{J}(n)$ At time n is a quadratic function of the tap-weight vector, so we can write,

$$\mathbf{J}(n) = \boldsymbol{\sigma}_{\mathbf{d}}^2 - \mathbf{w}^{\mathbf{H}}(n)\mathbf{p} - \mathbf{p}^{\mathbf{H}}\mathbf{w}(n) + \mathbf{w}^{\mathbf{H}}(n)\mathbf{R}\mathbf{w}(n) \quad (2)$$

Where $\boldsymbol{\sigma}_{\mathbf{d}}^2$ is variance of the desired response d(n) or $SINR(n+1)$, p is cross correlation vector between the tap-input vector $\mathbf{SINR}(n)$ and the desired response, and R is correlation matrix of the tap-input vector. According to the method of steepest descent, the updated value of the tap weight vector at time n+1 is computed by us ing recursive relation,

$$\mathbf{w}(n+1) = \mathbf{w}(n) + \frac{1}{2}\mu[-\nabla(n)] \quad (3)$$

Where μ is step size parameter or weighting constant. We get the following value for the gradient vector,

$$\nabla(n) = \frac{\partial \mathbf{J}(n)}{\partial \mathbf{w}(n)} = -2\mathbf{p} + 2\mathbf{R}\mathbf{w}(n) \quad (4)$$

We may compute the updated value of the tap weight vector $\mathbf{w}(n+1)$ by using recursive relation as the deterministic gradient algorithm.

$$\mathbf{w}(n+1) = \mathbf{w}(n) + \mu[\mathbf{p} - \mathbf{R}\mathbf{w}(n)] \qquad n = 0,1,2,\cdots \quad (5)$$

If it were possible to make exact measurement of the gradient vector at each iteration, and if the step-size parameter μ is suitably chosen, then the tap-weight vector computed by us ing the method steepest descent would indeed converge to the optimum weiner solution. In multi path fading channel, however, exact measurements of gradient vector are not possible, and the gradient vector must be estimated from the available data in mobile DS/CDMA signals. In other words, the tap-weight vector is updated in accordance with an algorithm that adapts to incoming data. One such algorithm is Least-Mean-Square (LMS) algorithm. A significant feature of the LMS algorithm its simplicity. It does not require measurements of the pertinent correlation functions, nor does it require matrix inversion. The simplest choice of estimator for R and p is to use instantaneous estimates that are based on s ample values of the tap-input vector and desired response, as defined by respectively,

$$\hat{\mathbf{R}}(n) = \mathbf{SINR}(n)\,\mathbf{SINR}^{\mathbf{H}}(n) \tag{6}$$

And

$$\hat{\mathbf{p}}(n) = \mathbf{SINR}(n)\,SINR(n+1) \tag{7}$$

Correspondingly, the instantaneous estimate of the gradient vector is as follows:

$$\hat{\nabla}(n) = -2\mathbf{SINR}(n)\,SINR(n+1) + 2\mathbf{SINR}(n)\,\mathbf{SINR}^{\mathbf{H}}(n)\,\hat{\mathbf{w}}(n) \tag{8}$$

Substituting the estimates of gradient vector ∇n the steepest-descent algorithm as described,

$$\hat{\mathbf{w}}(n+1) = \hat{\mathbf{w}}(n) + \mu\,\mathbf{SINR}(n)\left(SINR(n+1) - \mathbf{SINR}^{\mathbf{H}}(n)\hat{\mathbf{w}}(n)\right) \tag{9}$$

Equivalently, we may write the results in the form of apair relations as follows

$$e(n) = SINR(n+1) - \hat{\mathbf{w}}^{\mathbf{H}}(n)\mathbf{SINR}(n) \tag{10}$$

And

$$\hat{\mathbf{w}}(n+1) = \hat{\mathbf{w}}(n) + \mu\,\mathbf{SINR}(n)\,e(n) \tag{11}$$

The LMS algorithm is used in neural network as back propagation learning [35]. The diagram of the weight adaptation in neural network by back propagation learning algorithm is shown in Fig.3.

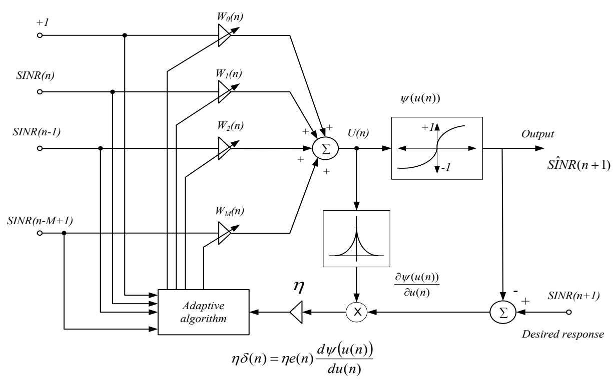

Fig.3 Diagram of back propagation learning algorithm

According to the method of back propagation learning algorithm, the weight updated as follows,

$$\hat{\mathbf{w}}(n+1) = \hat{\mathbf{w}}(n) + \mu\delta(n)\mathbf{SINR}(n) \tag{12}$$

Where $\delta(n)$ is learning signal or local error and we can write

$$\delta(n) = e(n)\psi'(u(n)) \tag{13}$$

Where $\psi'(u(n))$ is the derivative of the activate function $\psi(u(n))$. We can chose the sigmoid function as the activate function $\psi(u(n)) = \tanh(u(n))$ in neural network. So we can write

$$\psi'(u(n)) = \left(1 - \left(S\hat{I}NR(n+1)\right)^2\right) \tag{14}$$

and by substituting the $\psi'(u(n))$ in the back propagation algorithm as described in (12) ,

$$\hat{\mathbf{w}}(n+1) = \hat{\mathbf{w}}(n) + \mu e(n)\left(1 - \left(S\hat{I}NR(n+1)\right)^2\right)\mathbf{SINR}(n) \tag{15}$$

We use back propagation algorithm in offline and online learning as will be described in section 4.

3. Rayleigh fading power signal and SINR estimator

3.1 Rayleigh fading channel model.

One of the most commonly used methods to simulate a Rayleigh fading channel is described in [36] and is referred to as the Jake's method. A simplified channel simulator often assumes the superposition of plane waves, whose arrival angle are uniformly distributed and associated with different Doppler shifts, ranging from the minimum to the maximum specified by the mobile speed [37]. The Jake's method assumes that the line-of-sight component is absent. When the number of paths is large enough, the base band signal received from a multipath fading channel is approximately a complex Gaussian process and it invoke central limit theorem. We can write the amplitude fluctuation of the base band signal as follows

$$\beta(t) = \frac{1}{\sqrt{L}}\left\{\sum_{l=1}^{L/2-1}\left[e^{j2\pi(f_D Cos\psi_l t - f_c\tau_l)} + e^{-j2\pi(f_D Cos\psi_l t - f_c\tau_{-l})}\right] + e^{j2\pi(f_D t - f_c\tau_L)} + e^{-j2\pi(f_D t - f_c\tau_{-L})}\right\} \tag{16}$$

Here $\beta(t)$ is amplitude fluctuation, L is the number of paths and $\psi_l(t)$ has a uniform distribution in $[0,2\pi]$, and $\tau_l << T_s$ (T_s is the sample duration) in frequency-nonselective channel. In this paper, we implement Rayleigh fading simulator using 34 paths [36], [38]. Here we consider a slow fading channel and the fading factor is constant within the symbol duration. The simulated Rayleigh fading channel with a maximum Doppler-spread $f_D = 50\,HZ$ during a 200 ms period is shown in Fig.4. The fading channel described in Fig.4 can be experienced by a mobile which is traveling at 30 km/h when the carrier frequency is $f_c = 1.8\,GHZ$ and transmitting data at a symbol rate of 60 kbps. We can see in Fig.4. received signal fluctuation frequently drops far below its average level due to Rayleigh fading.

3.2 SINR estimation or measurement

The base station dispreads the received base band signal by the conjugate of the kth user’s spreading sequence and integrated over M chips.

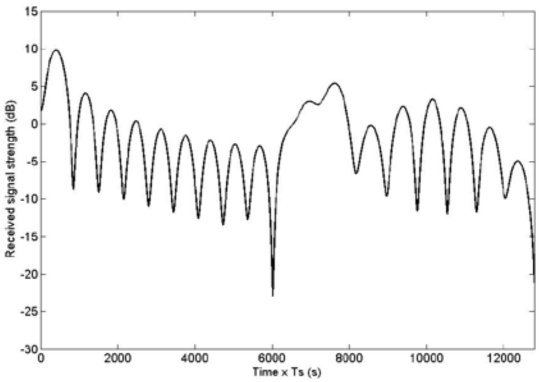

Fig.4.simulated Rayleigh fading ($f_D = 50Hz$, $T_s = 15.625\mu s$)

The jth user's signal strength is attenuated by the factor $1/M$ (cross correlation between spreading sequences) after dispreading by the kth user's spreading sequences [39], [40], [41]. The SINR of the kth user during one symbol period can be expressed as follows

$$\gamma_k(n) = \frac{|A_k \beta_k(n)|^2}{\frac{1}{M}\sum_{j \neq k} |A_j \beta_j(n)|^2 + \sigma_k^2(n)} \quad (17)$$

Here $\beta_k(n)$ is the fading channel coefficient and $\sigma_k(n)$ is the standard deviation of the Additive White Gaussian Noise (AWGN) experienced by the k[th] user. The data symbols are oversampled to obtain a larger number of observations. To simulate the uplink fading channels, an independent and uncorrelated Rayleigh fading for each user $\beta_k(n), k = 1,2,\ldots,12$ is generated using the Jake's method as described.

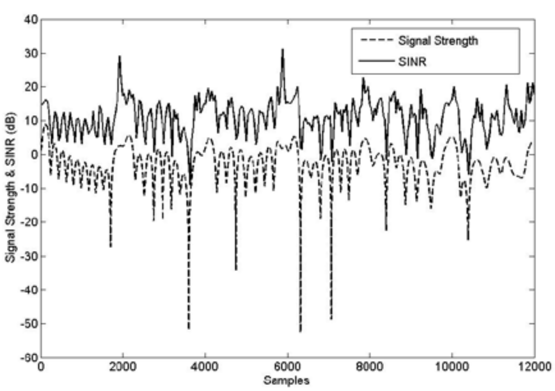

Fig.5 SINR in Rayleigh fading ($f_D = 17Hz$,with K=12)

The maximum Doppler spread is varied for each user from 17Hz to 170Hz to reflect different user's mobility.

$$f_D = 1.67 v_k \; Hz, \qquad v_k = 10.k \; km/h \quad (18)$$

We add the AWGN with the variance $\sigma_n^2 = 7dB$ below the signal power level (SNR=7dB).SINR measurement is performed in every time slot that corresponds to one power control interval $T_p = 0.667ms$. The simulated fading envelope for a v ehicle with speed of 120km/h and its corresponding SINR are shown in Fig.5. We used all data symbols in the time slot to estimate the SINR. The chip rate is assumed $R_c = 3.84\,Mcps$ as given in the 3G specification for uplink data channel. Therefore, 40 binary symbols per time slot are available for the SINR estimation.

4. Neural network-based predictor and optimization

4.1 MLP and Adaline predictors

Neural networks are well suited to be utilized as nonlinear predictive filters because of their distinguished approximation and generalization capabilities [42]. Consider a f eed forward multilayer perceptron as a predictive filter with one hidden layer. This MLP predictor with p input nodes and q h idden nodes $SINR(n), SINR(n-1),\ldots, SINR(n-p+1)$ is illustrated in Fig.6. The single node in the output layer represents the one-step-ahead prediction. The hyperbolic tangent sigmoid functions are used as the nonlinear transfer function of the hidden nodes and the transfer function of the output node is linear. The number of input nodes p and the number of hidden nodes should be optimized. There are two principles to find the optimal predictor and optimal p and q numbers. We use Adaline neural network as linear predictive filter. It has k input nodes $SINR(n), SINR(n-1),\ldots, SINR(n-k+1)$ and the single node in output layer. So it represents one-step-ahead prediction as illustrated in Fig.7. The transfer function in output node in Adaline predictor is linear. There are many ways to maximize the predictor generalization as will be described in part 4.2.

4.2 MLP and Adaline Predictors Optimization

From the network structure's point of view, we may select the optimal number of input and hidden nodes, or assume partial connection between different nodes and apply some pruning methods to eliminate very small weights in order to simplify the network structure [43], [44]. The number of hidden nodes q, in MLP model, and the number of input nodes in MLP and Adaline should be optimized. There are two principles to find the optimal predictor. Two criteria, minimum mean squared error (MSE) and minimum description length (MDL) criteria [30], [45] are used for filter design parameter selection. In this paper we used MSE principle to find the optimal structure or the length of predictor because MDL is actually a criterion to used for finding the order of the autoregressive (AR) process and our Rayleigh fading channel predictor is not an AR process therefore MDL criteria cannot be expected to give exact results. MSE principle is given as

$$MSE = \frac{1}{N}\sum_{n=0}^{N-1}\left[S\hat{I}NR(n+1) - SINR(n+1)\right]^2 \quad (19)$$

Here $x(n), n = 1,2,\ldots,N$ are the samples values of the time series to be predicted. We have

$$u_i(n) = \sum_{j=1}^{p} w_{ji}\, SINR(n-j) \qquad i = 1,2,\ldots,q \quad (20)$$

$$z_i(n) = \tanh[u_i(n)] \quad (21)$$

$$S\hat{I}NR(n+1) = \sum_{i=1}^{q} v_i z_i(n) + v_0 \quad (22)$$

We divided $\{\mathbf{SINR}(n)\}$ into $k_{\max} = \frac{N}{d}$ consecutive segments where d represents the length of prediction and $k_{\max}$ is an integer number.

We train each network with p inputs and q hidden nodes using the back propagation learning algorithm [46] to minimize the mean squared error in each segment

$$ES_{kd} = \sum_{n=kd}^{kd-1}\left[S\hat{I}NR(n+1) - SINR(n+1)\right]^2 \quad (23)$$

Then we use the obtained optimal weights and bias to predict the points $SINR(n+1), n = kd, kd+1,\ldots,(k+1)d-1$ in the following subsequent (k+1)th segment to maintain the actual mean squared prediction error

$$E_{(k+1)} = \frac{1}{d}\sum_{n=kd}^{kd-1}\left[S\hat{I}NR_{(k+1)}(n+1) - SINR_{(k+1)}(n+1)\right]^2 \quad (24)$$

In this prediction the parameters of the predictor are determined and updated using the past data. The predictions of the data points in the very first segment are taken as zero. This procedure is continued until the mean squared errors for all the segments are found. Then we calculate the total actual mean squared error as

$$E_{per} = E_{per}(p,q,d) = \frac{1}{(k_{\max}-1)}\sum_{k=1}^{k_{\max}-1} E_{(k+1)} \quad (25)$$

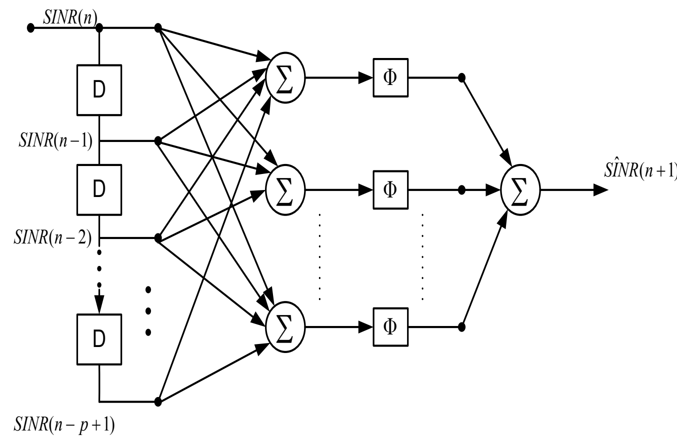

Fig.6 The structure of MLP neural network based predictor.

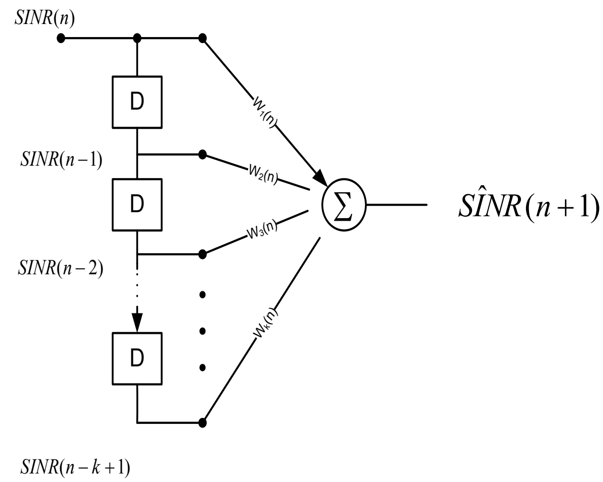

Fig.7 The structure of Adaline neural network based predictor

We find different E_{per} for the network with the p input nodes and q h idden nodes. We repeated the above procedure many times because the conventional back propagation is a deterministic optimization algorithm, and we found different mean squared errors in every trail. The final mean squared error of each mode was selected as the averaged mean squared error of all the experiments. when we repeated the above procedure for B times we got

$$\overline{E}_{per} = \overline{E}_{per}(p,q,d,B) = \frac{1}{B}\sum_{b=1}^{B} E_{per}(b) \quad (26)$$

Here b is the bth repetition. We select the network with the minimum $\overline{E}_{per}$ as the optimal predictor structure.

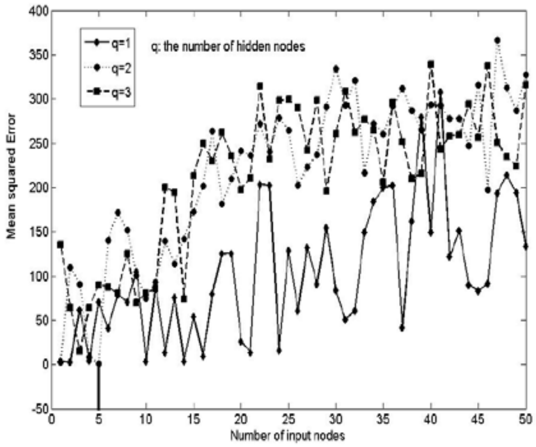

Fig.8. MSE of different MLP models at the speed of 10km/h.

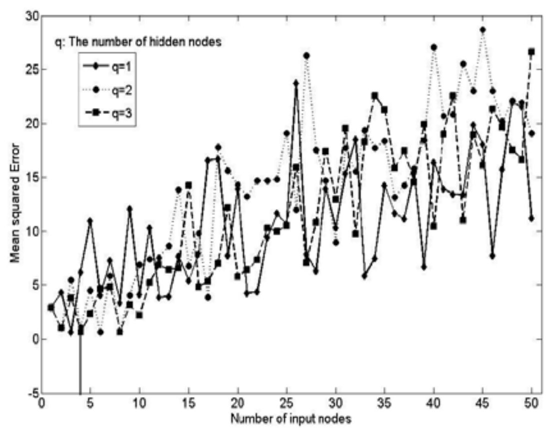

Fig.9. MSE of different MLP models at the speed of 60km/h.

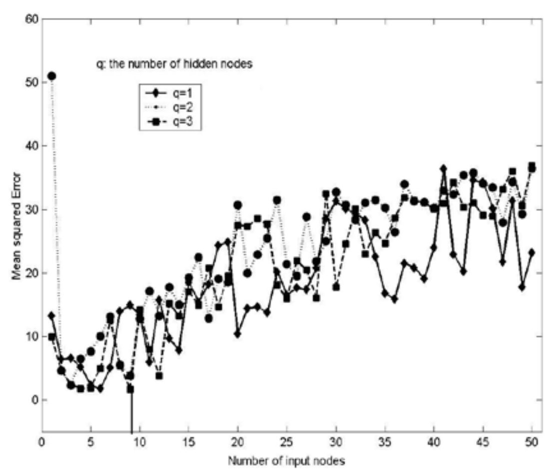

Fig.10 MSE of different MLP models at the speed of 120km/h

5. Simulation Results

5.1 Off-line optimization of MLP

Due to the time-varying and mobile speed-dependent characteristics of the power response of the Rayleigh fading channel, it is not practical to optimize predictor structure for a p ower signal covering the whole speed range [47], [49]. Therefore, we only consider the optimization of the network structures under three extreme conditions when the vehicle speed is 10, 60, 120 km/h. The additive noise is zero mean white Gaussian noise. We use $\mathbf{SINR}(n) = \{SINR(n), SINR(n-1), \ldots, SINR(n-p+1)\}$ from a segment of a received SINR, as shown in Fig.6 and Fig.7. This time series has 600 samples and the segment length d here is 200. In MLP predictor, the computational complexity will increase drastically by increasing the number of hidden nodes. A large number of hidden nodes is rarely used, and we change q in a s mall range, i.e. , q=1,2,3. The mean squared errors of different MLP structure for different vehicle speeds 10 km/h , 60 km/h and 120 km/h are given in Fig.8 , Fig.9 and Fig.10, respectively. The MLP with 5 input nodes and 2 hidden nodes turns out to be the best structure for the speed of 10 km/h. Similarly at the speed of 60 km/h the optimal MLP has 4 input nodes, and 3 h idden nodes and for vehicle's speed of 100km/h it has 9 input nodes and 3 hidden nodes. The MSE of all models candidates in Adaline at the speed of 10, 60, 120 km/h are given in Figs. 11, 12, 13, respectively. It is easy to find that the optimal Adaline has nine input nodes at the speed of 10 km/h, and for vehicle’s speed of 60 k m/h it has 5 i nput nodes, and with 18 input nodes turns out to be the best structure for the speed of 120 km/h.

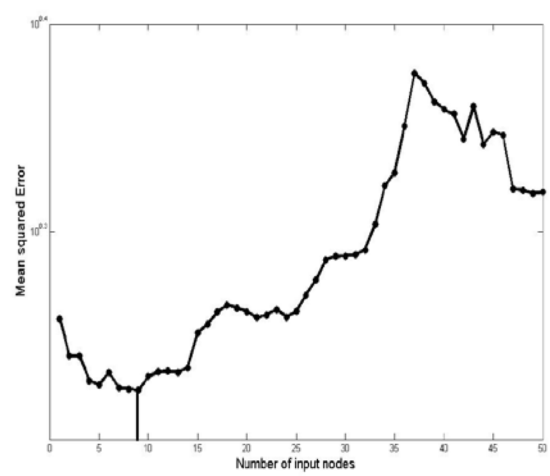

Fig. 11. MSE of different Adaline models at the speed of 10km/h

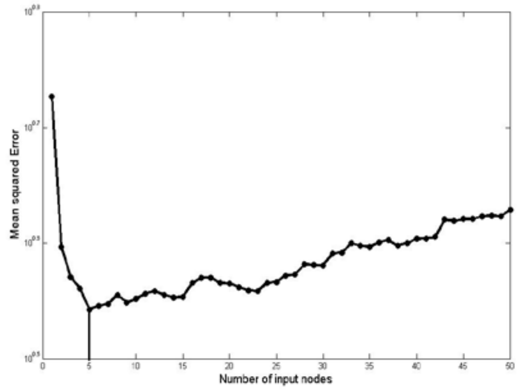

Fig.12 MSE of different Adaline models at the speed of 60km/h

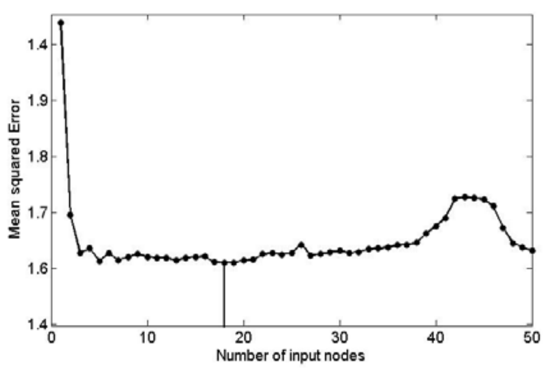

Fig.13 MSE of different Adaline models at the speed of 120km/h

5.2 Real time prediction with on-line adaptation

The optimal predictor obtained from the off-line procedure was then used with on- line adaptation because the fading signals were highly nonstationary [48]. We use an on-line back propagation algorithm to adapt new data quickly and adequately forgetting the old data .The structure of MLP and Adaline predictors are first optimized off-line using the procedure described above. The obtained optimal predictors are then used for prediction of SINR at the speeds of 10, 60, 120km/h. . The output of the optimal predictors at the speeds of 5 k m/h and 60km/h and 120km/h are shown in Figs. 14, 15, 16, respectively and the results show that the optimal MLP neural predictor can predict SINR with MSE values of about 0.02, 0.25 and 0.4 at the urban mobile speeds of 10 km/h, 60 km/h and 120 km/h respectively. The results show that the optimal MLP and Adaline predictors can predict SINR with the same MSE values of about 0.02, 0.25 at the urban mobile speeds of 10, 60 km/h, respectively. But by increasing the mobile velocity until 120km/h, the MSE value for Adaline predictor is 0.2 and this value for MLP predictor is approximately 0.4.

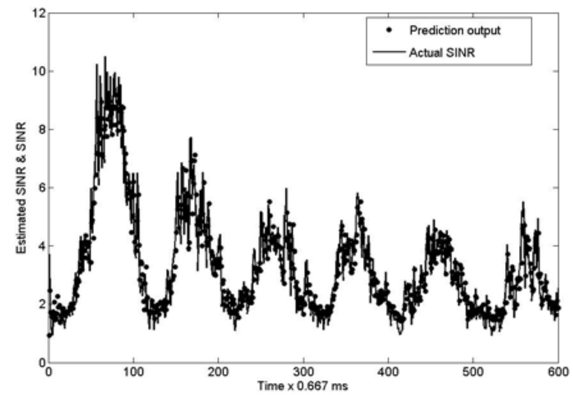

Fig.14 The prediction output of SINR at the speed of 10 km/h along with the actual SINR.

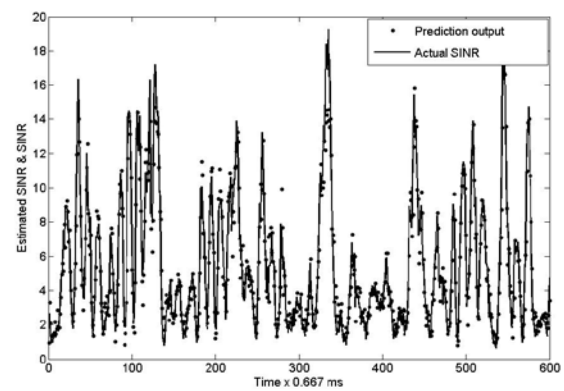

Fig.15 The prediction output of SINR at the speed of 60 km/h along with the actual SINR.

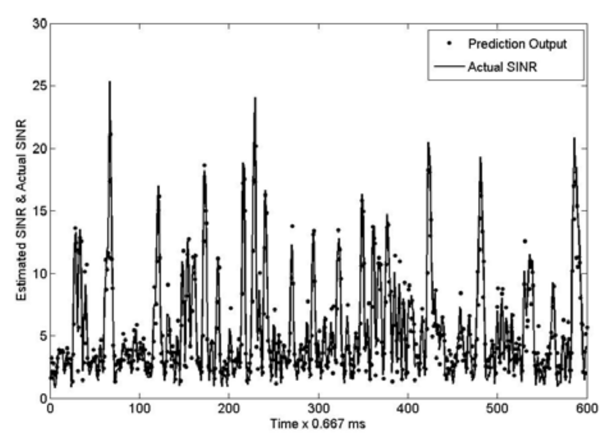

Fig.16 The prediction output of SINR at the speed of 100km/h along

6. Conclusion

We presented a MLP neural network-based single-step ahead SINR prediction scheme for reverse link power control in DS/CDMA systems. The neural predictor was optimized off-line using the MMSE method. The simulation results show that the Adaline predictor can estimates SINR with the same error as MLP when the user has the velocity of 5 km/h and 60 km/h but by increasing the velocity up-to 120 km/h the mean squared error of MLP is two times more than Adaline predictor. This makes the Adaline predictor (with lower complexity) more suitable than MLP for closed-loop power control.

References

[1] A. Wang, V. Krishnamurthy, "Mobility enhanced smart antenna adaptive sectoring for uplink capacity maximization in CDMA cellular network," IEEE Transactions on Communications, vol. 56, no. 5, May 2008 pp. 743-753.
[2] N. Benvenuto, G. Carnevale, S. Tomasin, "Joint power control and receiver optimization of CDMA transceivers using successive interference cancellation," IEEE Transactions on C ommunications, vol. 55, no. 3, March 2007 pp. 563-573
[3] S. Jagannathan, M. Zawodniok, Q. Shang, "Distributed power control of cellular networks in the presence of Rayleigh fading channel," IEEE INFOCOM 2004 - IEEE International Conference on C omputer Communications, no. 1, March 2004 pp. 1056-1067.
[4] W. Choi, C. Yi, J. Y. Kim, D. I. Kim, "A new base station receiver for increasing diversity order in a CDMA cellular system," IEEE Transactions on C ommunications, vol. 52, no. 11, Nov 2004 pp. 1851-1856.
[5] X. Wang, R. Ramjee, H. Viswanathan, "Adaptive and predictive downlink resource management in next-generation CDMA networks," IEEE Journal on S elected Areas in Communications, vol. 23, no. 6, June 2005 pp. 1219-1232.
[6] B. Chen, B. Lee, S. Chen, "Adaptive power control of cellular CDMA systems via the optimal predictive model," IEEE Transactions on W ireless Communications, vol. 4, no. 4, Jul 2005 .
[7] L. Zhao, Jon W. Mark, "Multi step closed-loop power control using linear receivers or DS-CDMA systems," IEEE Transactions on W ireless Communications, vol. 3, no. 6, Nov 2004 .
[8] H. J. Su and E. Geraniotis, "Adaptive closed-loop power control with quantized feedback and loop filtering," IEEE Trans. Wireless Commun., vol. 1, no. 1, pp. 76–86, Jan. 2002.
[9] F. Gunnarsson, F. Gustafsson, and J. Blom, "Dynamical effects of time delays and time delay compensation in power controlled DS-CDMA," IEEE J. Sel. Areas Commun., vol. 19, no. 1, pp. 141–151, Jan. 2001.
[10] M. D. Anderson and S. Perreau, "Robust power control for CDMA networks subject to modelization errors," in IEEE Int. Conf. Acoustics, Speech, and Signal Processing, 2003, Hong Kong, vol. 4, pp. 161–164.
[11] B. Lee, H. Chen, B. Chen, "Power control of cellular radio systems via robust Smith prediction filter," IEEE Transactions on Wireless Communications, vol. 3, no. 5, Sep 2004.
[12] T. W. Yoon, H. J. Kim, W. Kim, and C. Kang, "Adaptive minimum variance closed-loop power control in CDMA cellular systems," IEICE Trans. Commun., vol. E85-B, no. 1, pp. 210–220, Jan. 2002.
[13] L. Qian and Z. Gajic, "Variance minimization stochastic power control in CDMA systems," in Proc. Int. Conf. Communications (ICC) 2002, New York, pp. 1763–1767.
[14] K. Shoarinejad, J. L. Speyer, G. J. Pottie, "Integrated predictive power control and dynamic channel assignment in mobile radio systems," IEEE Transactions on Wireless Communications, vol. 2, no. 5, Sep 2003 pp. 976-988.
[15] W. Panichpattanakul, W. Benjapolakul ,"Fuzzy power control with weighting function in DS-CDMA cellular mobile communication system," in Int. Symp. Circuits and Systems, 2003 (ISCAS '03), Bangkok, Thailand, vol. 5, pp. 785–788.
[16] A. J. Viterbi, A. M. Viterbi, and E. Zehavi, "Performance of power controlled wideband terrestrial digital communication," IEEE Trans. On Vehicular Tech. vol. 41, no. 4, April 1993.
[17] L. Dong, G. Xu, Hao Ling, "Predictive downlink beamforming for wideband CDMA over Rayleigh-fading channels," IEEE Transactions on Wireless Communications, vol. 4, no. 2, Mar 2005.
[18] H. Su, E. Geraniotis, "Adaptive closed-loop power control with quantized feedback and loop filtering," I EEE Transactions on Wireless Communications, vol. 1, no. 1, January 2002.
[19] H. Jiang, W. Zhuang, X. Shen, "Quality-of-service provisioning and efficient resource utilization in CDMA cellular communications," IEEE Journal on Selected Areas in Communications, vol. 24, no. 1, January 2006 pp. 4-15.
[20] C. Lee, C. Chang, W. Sheen, "A capacity analysis method for uplinks in DS/CDMA cellular systems with imperfect SIR-based power control and multipath fading", IEEE Transactions on Wireless Communications, vol. 7, no. 1, January 2008.
[21] G. Yue, X. Zhou, X. Wang, "Performance comparisons of channel estimation techniques in multipath fading CDMA," IEEE Transactions on Wireless Communications, vol. 3, no. 3, May 2004.
[22] J. G. Andrews, T. H. Meng, "Optimum power control for successive interference cancellation with imperfect channel estimation," IEEE Transactions on Wireless Communications, vol. 2, no. 2, Mar 2003 pp. 375-383.
[23] X. Liu, E. Gunawan, "Interference identification and blind multi user detection for asynchronous CDMA systems with multipath fading," IEEE Transactions on Communications, vol. 55, no. 12, December 2007.
[24] J. Ling, U. Tureli, "Signal to interference prediction for adaptive radio links," GLOBECOM 2006 - IEEE Global Telecommunications Conference, no. 1, November 2006.
[25] F. Chiti, R. Fantacci, G. Mennuti, D. Tarchi, "Dynamic SIR based admission control algorithm for 3G wireless

networks", ICC 2003 – IEEE International Conference on Communications, no. 1, May 2003.

[26] J. Ling, U. Tureli, "SIR prediction for downlink packet access", MILCOM 2006 - IEEE Military Communications Conference, no. 1, October 2006, pp. 1782-1786.

[27] X. Z. Gao, X. M. Gao, and S. J. Ovaska, "A modified neural network model with application to dynamical systems identification," In proceeding of the 1996 I EEE International Conference on Systems, October 1996.

[28] Y. Chen, C. Chang, Y. Hsieh, "A channel effect prediction-based power control scheme using PRNN/ERLS for uplinks in DS-CDMA cellular mobile systems," IEEE Transactions on Wireless Communications, vol. 5, no. 1, January 2006.

[29] S. Chen, C. Yang and S. Li," Adaptive two-loop power tracking control in CDMA systems with the utility optimization," IEEE Transactions on Wireless Communications, vol. 7, no. 4, April 2008, pp. 1358 – 1368.

[30] X. M. Gao, X. Z. Gao, J. M. A. Tanskanen, and S. J. Ovaska, " Power prediction in mobile communication systems using an optimal neural-network structure," IEEE Trans. on Neural Networks, vol. 8, no. 6, November 1997.

[31] M. Shikh-Bahaei, "Joint optimization of "Transmission rate" and "Outerloop SNR target" adaptation over fading channels," IEEE Transactions on Communications, vol. 55, no. 3, March 2007 pp. 398-403.

[32] X. Wang, R. Ramjee, H. Viswanathan, "Adaptive and predictive downlink resource management in next-generation CDMA networks," IEEE Journal on S elected Areas in Communications, vol. 23, no. 6, June 2005 pp. 1219-1232.

[33] S. Haykin, Adaptive Filter Theory, Prentice-Hall information and system sciences series, 2008.

[34] J. G. Proakis, Digital Signal Processing, principles, algorithm and application, 2005.

[35] C. T. Leondes, Neural Network Systems Techniques and Applications, Algorithms and Architectures," 2008

[36] W. C. Jake, Microwave Mobile Communications, Newyork, Johnwilley, 1994.

[37] Y. R. Zheng, C. Xiao, "Simulation models with correct statistical properties for Rayleigh fading channels," IEEE Transactions on Communications, vol. 51, no. 6, Jun 2003 pp. 920-928

[38] B. Chen, J. Liao, "Adaptive MC-CDMA multiple channel estimation and tracking over time-varying multipath fading channels," IEEE Transactions on Wireless Communications, vol. 6, no. 6, June 2007.

[39] J. G. Proakis, Digital Communications, Newyork: McGraw-Hill, 2005.

[40] R. L. Peterson, R. E. Ziemer, and D. E. Borth, Introduction to Spread Spectrum Communications, Singapore, Prentice Hall international, 1995.

[41] A. J. Viterbi, Principles Of Spread Spectrum Communication, 1995.

[42] D. P. Mandic and J. A. Champers, Recurrent Neural Networks for Prediction Learning Algorithms Architecture and Stability, 2001.

[43] C. T. Leondes, Neural Network Systems Techniques and Applications, Optimization Techniques, 2008.

[44] Y. H. Hu, Hand Book of Neural Network Signal Processing, 2005.

[45] X. M. Gao, S .J. Ovaska, and I. O. Hartimo, "Restoration of noisy speech using an optimal neural network structure," IEEE International Conference on neural networks, vol. 8, no. 6, November 1997.

[46] A. Cichocki, and R. Unbehauen, Neural Networks for Optimization and Signal Processing, 1993.

[47] S. Aissa, J. Kuri, P. Mermelstein, "Call admission on the uplink and downlink of a CDMA system based on total received and transmitted powers," IEEE Transactions on Wireless Communications, vol. 3, no. 6, Nov 2004 pp. 2407-2416.

[48] H. Bang, T. Ekman, D. Gesbert, "Channel predictive proportional fair scheduling," IEEE Transactions on Wireless Communications, vol. 7, no. 2, February 2008 pp.482-487

[49] S. I. Gallant, Neural Network Learning and Expert System, 2008.